Electron density study of urea using TDS-corrected X-ray diffraction data: quantitative comparison of experimental and theoretical results

Valery Zavodnik,[a] Adam Stash,[a] Vladimir Tsirelson,[b] Roelof de Vries[c] and Dirk Feil[c]*

[a]*L. Karpov Institute of Physical Chemistry, Moscow 103064, Vorontsovo Pole 10, Russia,* [b]*D. Mendeleev University of Chemical Technology, Moscow 125047, Miusskaya Sq. 9, Russia, and* [c]*Chemical Physics Laboratory, Twente University, PB 217, 7500AE Enschede, The Netherlands. E-mail: feil@ct.utwente.nl*

Abstract

The electron-density distribution in urea, $CO(NH_2)_2$, was studied by high-precision single-crystal X-ray diffraction analysis at 148 (1) K. An experimental correction for TDS was applied to the X-ray intensities. $R_{merge}(F^2) = 0.015$. The displacement parameters agree quite well with results from neutron diffraction. The deformation density was obtained by refinement of 145 unique low-order reflections with the Hansen & Coppens [*Acta Cryst.* (1978), A**34**, 909–921] multipole model, resulting in $R = 0.008$, $wR = 0.011$ and $S = 1.09$. Orbital calculations were carried out applying different potentials to account for correlation and exchange: Hartree–Fock (HF), density-functional theory/local density approximation (DFT/LDA) and density-functional theory/generalized gradient approximation (DFT/GGA). Extensive comparisons of the deformation densities and structure factors were made between the results of the various calculations and the outcome of the refinement. The agreement between the experimental and theoretical results is excellent, judged by the deformation density and the structure factors [$wR(HF) = 0.023$, $wR(DFT) = 0.019$] and fair with respect to the results of a topological analysis. Density-functional calculations seem to yield slightly better results than Hartree–Fock calculations.

1. Introduction

Urea, $CO(NH_2)_2$, has been the subject of extensive theoretical and experimental studies in the past three decades, mainly because of its interesting physical and chemical properties (Worsham *et al.*, 1957; Mullen & Hellner, 1978; Scheringer *et al.*, 1978; Guth *et al.*, 1980; Swaminathan, Craven & McMullan, 1984; Swaminathan, Craven, Spackman & Stewart, 1984; Spackman *et al.*, 1988; Dovesi *et al.*, 1990; Boek *et al.*, 1991; Velders & Feil, 1993; Niu Jier, 1994; Gatti *et al.*, 1994; Dixon & Matzuzawa, 1994). Urea complexes easily with different molecules, possesses non-linear optical properties and seems to be the only example of a compound containing a carbonyl group involved in four hydrogen bonds. These studies are mainly devoted to the determination of accurate positional and displacement parameters, and the electron-density distribution (EDD). Experimental and quantum-chemical studies of the latter and occasionally a qualitative comparison have been carried out (Swaminathan, Craven, Spackman & Stewart, 1984).

The present study makes a quantitative comparison of the experimental and theoretical EDD of urea. Good agreement between the two is assumed to reflect the accuracy of the data and the quality of the calculations. As such, this study is a continuation of the work by Swaminathan, Craven, Spackman & Stewart (1984), with a number of improvements:

(i) the experimental data were corrected for TDS using a recently developed method;

(ii) several quantum-chemical methods were employed, all including the effects of the crystalline environment;

(iii) the comparison is quantitative with respect to the structure factors.

We have calculated the EDD and structure factors from crystal orbitals obtained by solving the Fock equations with the Hartree–Fock and various density-functional theory (DFT) potentials. Comparison of structure factors is important for three reasons. Firstly, the magnitudes of the structure factors are directly related to the net intensities and as such are the most suitable quantities to be compared with theory. Secondly, since the phases of the structure factors cannot be observed, the experimental EDD has a fundamental uncertainty arising from the uncertainty in the phases used. Thirdly, molecular interaction affects the diffuse EDD in the intermolecular region. This is hardly visible in electron-density plots, but shows up clearly in the low-order region in reciprocal space.

2. Experimental

Single crystals of urea were grown from aqueous solution by slow evaporation of the solvent. The carefully chosen sample used in the X-ray diffraction study was $0.30 \times 0.30 \times 0.35$ mm with (110) and (100) planes as surfaces. Measurements were performed using a Syntex $P\bar{1}$ four-circle automatic X-ray diffractometer with

Table 1. *Crystal and experimental data for urea*

	293 K	148 K
Space group		$P\bar{4}2_1m$
a (Å)	5.660 (1)	5.5890 (5)
c (Å)	4.7119 (7)	4.6947 (4)
V (Å^3)	150.95 (8)	146.64 (4)
μ (cm^{-1})		1.27†
$(\sin\theta/\lambda)_{max}$ (Å^{-1})	0.99	1.15
Scan angle ω (°)		$0.7 + 0.345\tan\theta$
Counter aperture (°)		0.9
No. of measured reflections	1473	1971
No. of unique reflections	271	412
$R_{int}(F^2)$	0.02	0.015
R_σ‡	0.005	0.005
a_2, a_3 [see (6) in Appendix A]	0.188, 0.073	0.144, 0.000

† This value was used instead of the more correct value of 1.17 cm^{-1}.   ‡ $R_\sigma \equiv (2/\pi)^{1/2}\{\Sigma\sigma[F(\mathbf{h})]/\Sigma F(\mathbf{h})\}$.

β(Nb)-filtered Mo $K\alpha$ radiation (0.7069 Å). The temperature was kept at 148 (1) K using a low-temperature (N$_2$) Syntex LT-1 attachment. The sample temperature was controlled using a thermocouple placed in the N$_2$ stream 30 mm from the crystal. The thermocouple was calibrated using another thermocouple placed in the center of the goniometer.

Urea crystallizes in the space group $P\bar{4}2_1m$ and the molecules lie at special positions with symmetry *mm*2. The unit-cell parameters were determined using reflections in the range $47 < 2\theta < 48°$. An ω–2θ scan was used for measuring the intensities of reflections in the four quadrants of reciprocal space. The intensities of three control reflections were monitored every 100 reflections and varied less than 1.5% during the experiment. All reflections, including weak reflections, were measured up to $\sin\theta/\lambda = 0.7$ Å^{-1}. Subsequently, reflections with intensities $I > 6\sigma(I)$ were measured in the interval $0.7 < \sin\theta/\lambda < 1.15$ Å^{-1}. Crystal data and experimental details are given in Table 1.

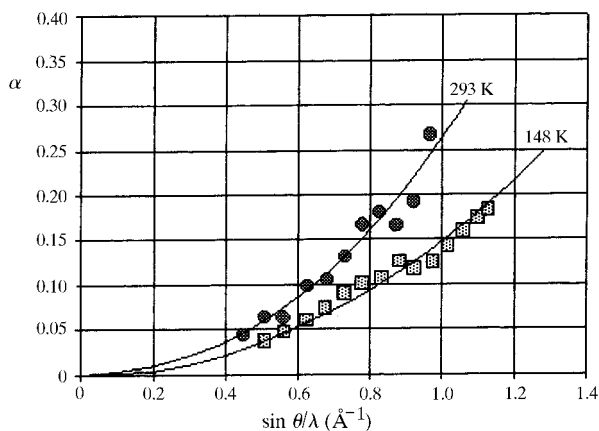The elastic constants for urea have not been measured to our knowledge. We therefore corrected the

Fig. 1. The experimental dependence of the TDS constant α of urea at 293 and 148 K as function of $\sin\theta/\lambda$.

Table 2. *Some results of the spherical-atom refinement of urea carried out on* $|F|$ *at 148 K*

No. of unique reflections (FA)†	412
No. of unique reflections (LA)	146
No. of parameters	28
Extinction correction (FA)	Secondary (Zachariasen, 1967)
Mosaicity (FA) (″)	11.2
R (FA)	0.025
wR (FA)	0.028
S (FA)	1.64
R (HA)	0.019
wR (HA)	0.023
S (HA)	1.18

† FA: full-angle refinement; HA: high-angle refinement, $\sin\theta/\lambda \geq$ 0.6 Å^{-1}; LA: low-angle refinement, $\sin\theta/\lambda < 0.6$ Å^{-1}.

measured X-ray intensities at 148 K for TDS using the Stash & Zavodnik (1996) experimental method (see Appendix A). To check the TDS correction method, we repeated the X-ray diffraction experiment using the same urea crystal at room temperature (see Table 1) and found the coefficients α [see (5) in Appendix A] to be approximately linearly dependent on the temperature (Fig. 1), as predicted by theory based on the harmonic approximation (Tsarkov & Tsirelson, 1991).

The total set of measured low-temperature intensities was corrected for TDS and (numerically) for absorption, and averaged over symmetry-equivalent reflections. The internal R factor, R_{merge}, was 0.015. The set of 412 symmetry-independent reflections was then used in the refinement procedure.†

3. Refinement and results

3.1. Spherical-atom refinement

The structure of urea was refined first by the full-matrix least-squares method using the spherical-atom model. The corresponding relativistic scattering factors and anomalous-scattering corrections were taken from *International Tables for Crystallography* (1995, Vol. C). The atomic displacements were modeled using the anisotropic harmonic approximation. Isotropic secondary extinction corrections calculated according to the Becker & Coppens (1974) and the Zachariasen (1967) formalisms resulted in the same deformation EDD maps. Therefore, the simpler Zachariasen model was applied. The secondary extinction in the crystal studied did not appear to be severe at either temperature, except for the 110 reflection for which the isotropic extinction correction factor y was 0.88. The program system *CSD* (Akselrud *et al.*, 1990) was used for these calculations.

Refinement was based on $|F|$ with least-squares weights equal to $1/[\sigma^2_{count}(F) + 0.000115F^2]$ (the first term

† Supplementary data for this paper are available from the IUCr electronic archives (Reference: SH0102). Services for accessing these data are described at the back of the journal.

Table 3. *Experimental (exp.) and modeled (calc.) displacement tensor components, $U^{ij} \times 10^4$ ($\mathring{A}^2$), based on the rigid-body model (148 K), compared with the data (N) extrapolated to the same temperature from the neutron diffraction results of Swaminathan, Craven & McMullan (1984)*

		$U^{11} = U^{22}$	U^{33}	U^{12}	$U^{13} = U^{23}$
C	exp.	167 (1)	86 (1)	−1 (1)	0
	N	172 (6)	80 (4)	1 (4)	0
	calc.	167	81	−3	0
O	exp.	220 (2)	79 (1)	24 (1)	0
	N	223 (7)	80 (4)	20 (5)	0
	calc.	220	81	24	0
N	exp.	317 (2)	113 (1)	−163 (1)	3 (1)
	N	330 (6)	115 (3)	−172 (3)	3 (3)
	calc.	317	113	−162	1
H1	N	486 (13)	224 (9)	−243 (9)	−29 (8)
	calc.	484	183	−325	−15
H2	N	470 (12)	158 (7)	−178 (9)	18 (8)
	calc.	486	113	−303	21

accounts for counting statistics and the second term is an empirical addition). The scale factor and extinction parameter were determined using both full- and low-angle ($\sin\theta/\lambda < 0.6$ $\mathring{A}^{-1}$) reflections, while the positional parameters and atomic displacement tensor elements of the non-H atoms were refined using the high-angle reflections ($\sin\theta/\lambda > 0.6$ $\mathring{A}^{-1}$). The procedure was repeated a few times iteratively. The 'contracted' H-atom *f* curve of Stewart *et al.* (1965) was used. In order to model the H atoms more realistically, the N—H bond distances were elongated to the neutron diffraction value (Swaminathan, Craven & McMullan, 1984) and librational analysis based on the rigid-body model (*International Tables for Crystallography*, 1995, Vol. C) was applied to the urea molecule. The *SHELXTL* system (Sheldrick, 1981) was used for this. The results are shown in Tables 2, 3 and 4.

Table 3 shows that the calculated components of the U^{ij} tensors of the non-H atoms are in very good agreement with the experimental values obtained by Swaminathan, Craven & McMullan (1984). The anisotropic displacement parameters of the H atoms were calculated from the results of the librational analysis. The structural parameters of the H atoms were then fixed and the other parameters of the structural model were refined again.

It is useful to compare the anisotropic displacement parameters of the H atoms determined by the rigid-body analysis to those predicted by extrapolation of the 12, 60 and 123 K neutron diffraction data to 148 K. This comparison (Table 3) shows good agreement and supports the procedure used to obtain the H-atom displacement parameters.

3.2. Multipole refinement

The program *MOLDOS*96 (Protas, 1995), based on the Hansen & Coppens (1978) multipole model, was

Table 4. *Librational (**L**), translational (**T**) and correlation (**S**) tensor components for urea at 148 K ($R_g = 0.006$)*

L (rad^2)

0.0058 (1)	0.0033 (0)	0.0000 (1)
	0.0058 (1)	0.0000 (1)
		0.0151 (1)

T ($\mathring{A}^2$)

0.0163 (1)	0.0012 (1)	0.0000 (1)
	0.0163 (1)	0.0000 (1)
		0.0081 (1)

S ($\mathrm{rad}\,\mathring{A}$)

−0.0023 (1)	0.0000 (0)	0.0000 (1)
0.0000 (0)	0.0023 (1)	0.0000 (1)
0.0000 (1)	0.0000 (1)	0.0000 (1)

Table 5. *Positional atomic parameters of urea obtained from the high-angle refinement of the spherical-atom model at 148 K (X) compared with those obtained from neutron diffraction data at 123 K (N) by Swaminathan, Craven & McMullan (1984)*

		x	y	z
C	X	0	1/2	0.3283 (1)
	N	0	1/2	0.3286 (2)
O	X	0	1/2	0.5963 (1)
	N	0	1/2	0.5965 (2)
N	X	0.1447 (1)	$x + 1/2$	0.1784 (1)
	N	0.1443 (1)	$x + 1/2$	0.1791 (1)
H1	X	0.2552	$x + 1/2$	0.2845
	N	0.2552 (4)	$x + 1/2$	0.2845 (4)
H2	X	0.1428	$x + 1/2$	−0.0339
	N	0.1428 (4)	$x + 1/2$	−0.0339 (3)

used for further refinement. The radial parameters, κ, the populations of the multipole functions (up to octa-poles for N and O, hexadecapoles for C and up to dipoles for H) and an extinction parameter according to

Zachariasen (1967) were varied. The atomic displacement parameters and the scale factor were fixed at the values obtained from the spherical-atom model refinement. In order to determine the range of structure factors to be used in the refinement, partial R factors averaged in small intervals (5–10°) of the diffraction angle θ (Fig. 2) and the corresponding partial 'error' R factors R_σ (see Table 1) were calculated.

As can be seen from Fig. 2, the spherical-atom model describes the EDD in urea properly only for the range of reflections with $\sin\theta/\lambda > 0.7$ Å^{-1}. Therefore, the 145 reflections with $\sin\theta/\lambda \leq 0.7$ Å^{-1} were used in the multipole model refinement. The partial R factors now became closer to the R_σ factors in the same interval. Special attention was paid to the correct determination of the scale factor. In each step of the refinement the ratio $k' = \Sigma F_{obs}(\mathbf{H})/k\Sigma F_{calc}(\mathbf{H})$ was calculated for small

Table 6. *Kappa values, κ, and atomic charges, q (a.u.), of the pseudo atoms*

	C	O	N	H
κ	0.97 (1)	0.98 (1)	0.98 (1)	1.02 (2)
q	4.03 (13)	6.23 (7)	5.30 (9)	0.79 (4)

intervals in θ. Fig. 3 shows that the scale factor determined using the spherical-atom model, as described above, gave the proper value. The results of the multipole refinement have been deposited as supplementary material.† The atomic charges and κ values are presented in Table 6.

We found excellent agreement between the observed structure factors and those based on the refined model: $R = 0.008$, $wR = 0.011$. This shows the level of noise to be low.

3.3. Deformation density

The most interesting planes are the plane of the molecule and the plane perpendicular to it, which contain the σ and π hydrogen bonds, respectively (see Fig. 4). Fortunately, both bonding regions are displayed in one cross section by two neighboring molecules. The reference state of the H atoms corresponding to the 'contracted' H-atom f curve of Stewart *et al.* (1965) was used. The static deformation density was obtained from the multipole functions using the program *SALLY* (Hansen, 1996). The result is shown in Fig. 5(*a*) for the plane that contains all intra- and intermolecular bonds. To estimate the effect of the TDS correction, we also performed a multipole analysis on the uncorrected data. The same refinement strategy was used. The refinement indices were $R = 0.008$, $wR = 0.011$ and $S = 1.09$; in other words, from a formal point of view the same minimum of the least-squares functional has been achieved. However, the resulting parameter values are different. The consequence for the deformation electron-density map can be judged from Fig. 5(*b*). The peak values in the C—N and N—H bonds increased by about 0.1 to 0.2 e Å^{-3} compared to the TDS-corrected values. The increase in density of the lone pairs of the O atom is even more significant.

As was stated earlier, urea has been analyzed before at 123 K by Swaminathan, Craven, Spackman & Stewart (1984). A straight comparison between the two studies is difficult since the present experiment was carried out at a different temperature and yielded more reflections. However, we can take the deformation parameters from their refinement and calculate the static structure factors using the nuclear coordinates of the present study. The difference between these structure factors and the structure factors derived from the present model is represented by partial R factors in Fig. 6. The considerable discrepancy observed is due to a number of
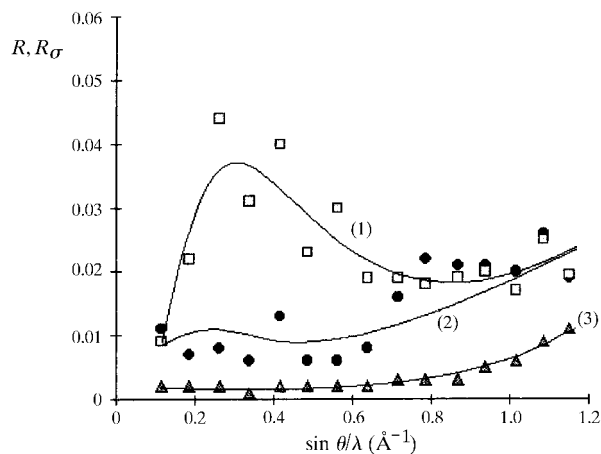

Fig. 2. Partial R factors (see §3.2) as function of $\sin\theta/\lambda$. (1) Spherical-atom refinement. (2) Multipole refinement. (3) The 'error' R factor R_σ (defined in Table 1).
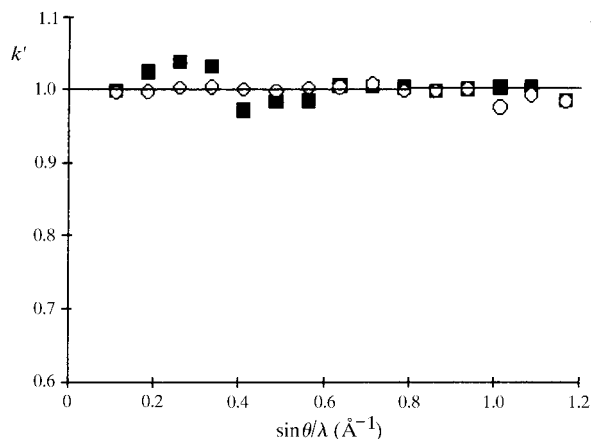

Fig. 3. The distribution of the ratio of observed to calculated structure factors, averaged over small intervals in $\sin\theta/\lambda$ (see §3.2). Circles: spherical-atom refinement; squares: multipole refinement.

---

† See deposition footnote on p. 46.

factors. Firstly, the noise has been removed by the multipole refinement in both sets of structure factors. A part of it, however, is absorbed by the deformation parameters causing a difference in the static EDD. Secondly, a correction for TDS was not applied by Swaminathan, Craven, Spackman & Stewart (1984); this is usually assumed to result in a bias in the displacement parameters. Since the decoupling of the displacement and deformation parameters is never perfect, this bias may contribute to the differences as well. Thirdly, the uncertainty in the phases of the reflections will influence the values of the structure factors of the model.

The dipole moment of the urea molecule in the crystal, calculated from our multipole parameters, is 3.8 D ($1 \, D \simeq 3.33564 \times 10^{-30} \, C \, m$). It is in good agreement with the results from gas and solution data of 3.8–4.6 D (Spackman *et al.*, 1988).

4. Comparison with theoretical results

4.1. Quantum-chemical electron-density calculations

A few years ago, urea was studied by Dovesi *et al.* (1990) by the three-dimensional periodical Hartree–Fock method implemented in the program *CRYSTAL* (Dovesi *et al.*, 1989). They used a 6-21G** basis set. Because Bloch functions with different **k** values were used, this was a rather large basis set and the addition of more diffuse functions would lead to numerical instability. Their study reports the EDD and the inter-action density due to hydrogen bonding. Since then a new version of the program, *CRYSTAL*95 (Dovesi *et al.*,

1996), has been developed. *CRYSTAL*95 can be used to carry out orbital calculations based on Hartree–Fock theory and also density-functional theory (DFT), with a choice of various approximations to the exchange-

(*a*)

(*b*)

Fig. 5. The static multipole density resulting from a Hansen–Coppens refinement with contracted H atoms. Contours are at intervals of 0.0675 e Å^{-3}. Negative contours are dashed. (*a*) Map calculated with TDS-corrected data. (*b*) As (*a*) but without a TDS correction.
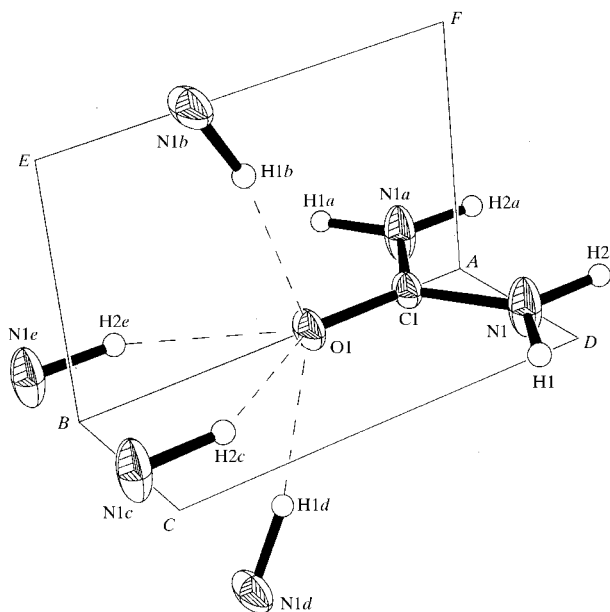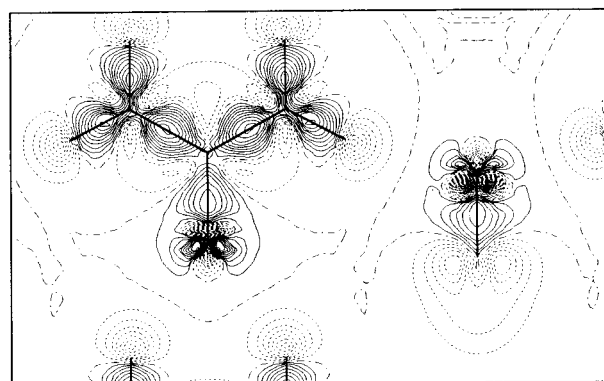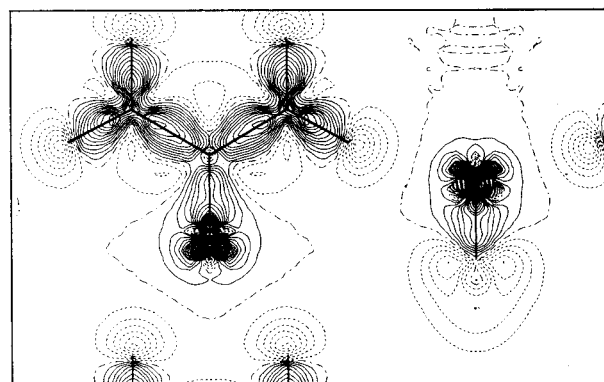
Fig. 4. The atom numbering and the hydrogen bonds in the urea crystal. Displacement ellipsoids are shown at the 50% probability level for non-H atoms.
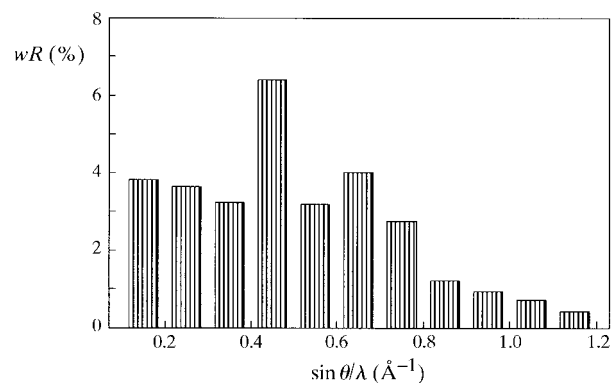
Fig. 6. Partial *R* factors as function of $\sin \theta / \lambda$ showing the difference between the static model structure factors obtained from experiments in this work and in the work of Swaminathan, Craven, Spackman & Stewart (1984).

correlation potential. The program can calculate EDDs and structure factors, both referring to the static structure. This allowed us to carry out a more extensive study than Swaminathan, Craven, Spackman & Stewart (1984) by taking molecular interactions into account.

The exchange-correlation potential based on the local density approximation (LDA) is widely applied. The results with respect to quantities of importance in chemistry, such as binding energy and bond distances, are disappointing. Within the last ten years or so, the gradient-corrected or generalized gradient approximation (GGA) potentials, which include the gradient of the density as well as the density itself, have been proposed and great improvements have been obtained (see *e.g.* Salahub *et al.*, 1995). As we obtained almost identical results for similar studies with different GGA potentials we include only one of them. Thus, we are left with two DFT calculations, using the following potentials:

(i) correlation according to a parameterization of the Ceperly–Alder free-electron gas correlation results (Vosko *et al.*, 1980) and LDA exchange potential (Dirac, 1930);

(ii) Perdew–Wang correlation (Perdew & Wang, 1986, 1989, 1992) and Becke exchange potential (Becke, 1988).

In our calculations we used the same basis set as Dovesi *et al.* (1990) and the same six **k** points in reciprocal space. The R factors expressing the difference between the sets of structure factors calculated with these theoretical methods are shown in Fig. 7. The difference between the two is smaller than the error in the experimental quantities. This leaves two quantum-chemical results, Hartree–Fock and DFT/GGA, to be compared with experiment. Fig. 7 suggests that the difference between the two may well be significant.

4.2. Comparison of theory and experiment

The experimental results refer to vibrating molecules in the crystalline state. The refinement shows that individual anisotropic displacement factors are necessary to
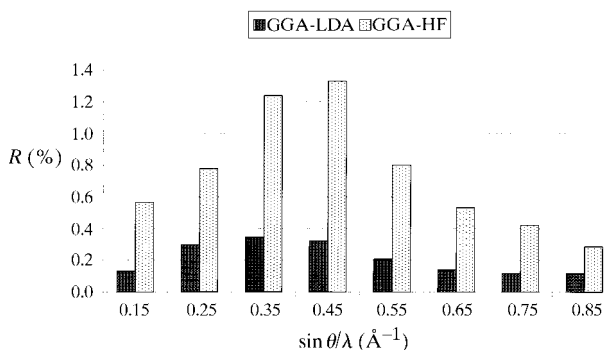
Fig. 7. Partial R factors as function of $\sin\theta/\lambda$ expressing the difference between structure factors calculated by various quantum-mechanical methods: HF, DFT/LDA and DFT/GGA.

model the system. Since we wish to compare theory and experiment as close as possible to the experimental situation, thermal motion has to be applied to the theoretical EDD and the corresponding structure factors. This was performed using the program *FITTER* (Bruning & Feil, 1992), which is based on the following considerations. The EDD close to a nucleus rigidly follows the thermal motion of that nucleus. The situation in the bonding region in between the nuclei is less clear, but calculations on the simple CO_2 molecule show that the assumption of rigid following can be applied to atoms obtained by the stockholder partitioning scheme (Hirshfeld, 1977), even for displacements corresponding to very high temperatures (unpublished results). *FITTER* first partitions the EDD into atoms with diffuse boundaries and then models these atoms with the help of a highly extended set of deformation functions very much greater in size than the set of functions used in crystallographic refinement of experimental data. The functions are Fourier transformed and individual thermal motion is applied. Numerical errors are small and no bias is introduced. The quality of *FITTER* modeling of the EDD is shown by the very low R factor of 0.0018 between the set of structure factors calculated by *CRYSTAL* and those resulting from the *FITTER* procedure in which no thermal motion is applied. This is to be compared with an R factor of *circa* 0.005 obtained by refining theoretical data with the standard refinement programs.

In the multipole refinement of experimental structure factors, the main objectives are the removal of noise and the deconvolution of thermal motion and deformation due to bonding. The first objective rules out the use of a large set of deformation functions. As a consequence some bias is introduced. Assuming the theoretical and the experimental sets of structure factors to be closely similar, we expect the introduction of the same bias when the theoretical structure factors, obtained using *FITTER*, are subjected to the same refinement procedure. Therefore, from the sets of HF and DFT structure factors the same 145 low-order reflections were selected as were used in the refinement of the experimental data discussed above. In a subsequent *MOLLY* refinement the positions and displacement parameters were kept at the experimental values and the scale factor was fixed to 1. The experimental weights were used throughout. The R factors expressing the difference between the original theoretical structure factors and the modeled structure factors are practically the same for both sets: $R = 0.005$ and $wR = 0.008$. The static deformation densities resulting from the refinements of the HF and DFT data, treated in the same way as the density shown in Fig. 5, are shown in Figs. 8(*a*) and 8(*b*), respectively. We notice the remarkable agreement between the two density distributions, confirming the results shown in Fig. 7. The major difference is found in the p_z region of the C atom, where the HF calculation shows more depletion. This

feature is most clearly expressed in the occupation of the quadrupole-moment function of the C atom pointing in the direction perpendicular to the plane of the molecule. The values found are −0.057 (7) *versus* −0.036 (7) for HF and DFT, respectively.

The results can be compared with the outcome of the refinement of the experimental data as shown in Fig. 5. We note the excellent agreement with the results based on the TDS-corrected data. The effect of the TDS correction is clearly seen in the region of the O atom; it is here where the theoretical distributions most clearly confirm the TDS correction method. The experimental distribution seems to agree better with the HF distribution, in particular in the region of the C atom discussed above.

A quantitative estimate of the difference between the experiment and each of the two models, HF and DFT, is given by the *wR* factors *wR*(HF) = 0.023 and *wR*(DFT) =
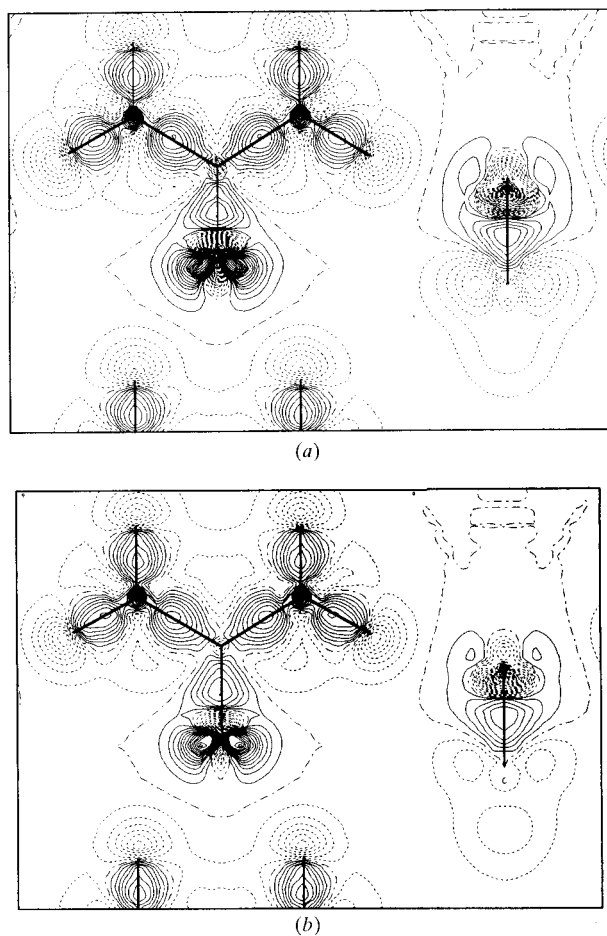

(a)

(b)

Fig. 8. Theoretical deformation density according to (a) the Hartree–Fock method and (b) the DFT/GGA method. In both cases the calculated EDD was transformed into structure factors, which in turn were subjected to a Hansen–Coppens refinement with contracted H atoms. The resulting multipole densities, obtained in the same way as in Fig. 5, are displayed. Contours are as in Fig. 5.

0.019. Fig. 9 expresses the same in terms of partial *R* factors. The DFT result is seen to agree better with experiment throughout reciprocal space with the exception of the very low order region, where only six structure factors are involved. Comparisons in reciprocal and in direct space are complimentary: the differences in the diffuse regions are not seen in the EDD maps, but are clearly observable in the low-order structure factors. We therefore stress that quantitative comparison between theory and experiment should include comparison of the structure factors in the various regions of reciprocal space.

The agreement between the experimental and theoretical results suggests that both the experimental study and the quantum-chemical calculations are quite accurate. Thus, in principle, it is feasible to undertake an experimental study of the interaction density, *i.e.* to calculate the difference between the experimental EDD of the crystal and the superposition of the (theoretical) EDDs of non-interacting molecules. When the results of such a study turned out to be disappointing, the multipole-refinement methodology was put under close scrutiny. It turned out that in the case of a non-centrosymmetric crystal, the phases of the structure factors obtained from a multipole refinement of noise-added data differ slightly from the real phases. These small phase differences, however, lead to errors in the structure factors of the crystal comparable in magnitude to the Fourier transforms of the interaction density (de Vries, 1996).

4.3. Topological characteristics of crystalline urea

The topological theory of EDD (Bader, 1990) claims that the critical points in the electron density, *i.e.* the points where $\nabla \rho = 0$, contain important chemical information. Among them are bond critical points, defined as points with a positive curvature (λ_3) along the atomic interaction line and two negative curvatures ($\lambda_1 < \lambda_2$) in the perpendicular directions. They are associated with 'share-type' interaction (covalent bonding) if
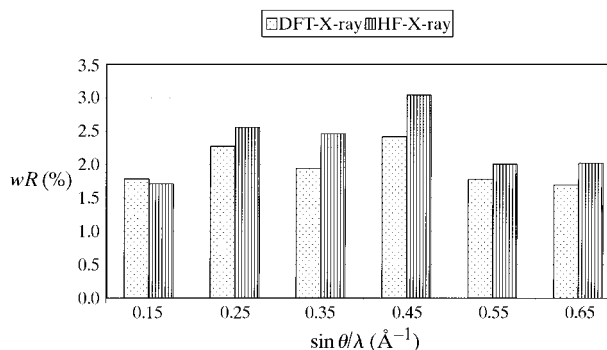

Fig. 9. Partial *R* factors reflecting the difference between the experimental and the modeled theoretical structure factors. The weight factors are derived from experiment.

Table 7. *The (3, −1) critical points in a urea crystal*

The modeled experimental and theoretical values are presented in the first and second lines, respectively.

Bond	R (Å)	ρ_b (e Å^{-3})	λ_1 (e Å^{-5})	λ_2 (e Å^{-5})	λ_3 (e Å^{-5})	$\nabla^2\rho$ (e Å^{-5})	ε	R_b (Å)
C—O	1.258	2.536	−23.33	−20.23	24.71	−18.86	0.15	0.427
	1.261	2.568	−24.97	−24.97	42.02	−7.923	0.003	0.411
C—N	1.343	2.538	−27.34	−23.00	12.68	−37.66	0.19	0.440
	1.345	2.352	−21.13	−19.21	12.73	−27.61	0.099	0.451
N—H1	1.005	1.797	−26.77	−25.54	21.88	−30.44	0.05	0.795
	1.009	2.319	−34.81	−33.13	21.13	−46.82	0.047	0.787
N—H2	0.997	1.843	−28.13	−26.93	21.68	−33.37	0.05	0.791
	1.005	2.352	−34.81	−33.37	20.89	−47.30	0.048	0.782
O···H1	2.014	0.159	−0.62	−0.57	2.77	1.58	0.09	1.269
	1.992	0.148	−0.72	−0.72	2.88	1.68	0.072	1.293
O···H2	2.071	0.142	−0.53	−0.52	2.58	1.53	0.02	1.275
	2.058	0.128	−0.48	−0.48	2.64	1.68	0.036	1.299

the Laplacian of the electron density ($\nabla^2\rho = \lambda_1 + \lambda_2 + \lambda_3$) is negative at these points and with ionic type interaction otherwise. Gatti *et al.* (1994) showed the influence of the crystalline environment on the curvatures by calculating the topological characteristics of a single molecule of urea and crystalline urea by the Hartree–Fock method (6-21[**] basis set). Whether an experimental EDD shows these characteristics depends, of course, on the quality of the data. Using the multipole model parameters, we have calculated the same values for crystalline urea based on the experimental electron density with a program developed by Howard & Mallinson (1993).

The experimental and theoretical values are presented in Table 7. We can conclude that there is semi-quantitative agreement between the experimental and theoretical topological characteristics of the intramolecular and intermolecular interactions.

5. Conclusions

The TDS correction applied in the present study showed a high degree of internal consistency when the corrections for low-temperature and room-temperature data were compared. The level of noise in the experimental data is low as is witnessed by an excellent agreement between the observed structure factors and those calculated from the refined model. The EDD and the structure factors resulting from a multipole modeling of the data were compared with the outcome of *CRYSTAL* calculations, modeled in the same way. The EDDs calculated with the density-functional method, with various potentials to account for correlation and exchange, did not show much mutual difference. They all resemble the EDD calculated by a Hartree–Fock *CRYSTAL* calculation. Both agree very well with the experimental EDDs, the TDS-corrected distribution yielding the better agreement. Whereas a qualitative comparison of the theoretical and the experimental deformation maps suggested the Hartree–Fock distribution to be the better one, a quantitative comparison of structure factors resulted in a clear preference for the density-functional method. Topological analysis showed

a fair agreement between theory and experiment. Uncertainty in the phases of the structure factors precludes the determination of the interaction density in the non-centrosymmetric urea crystal.

APPENDIX A

The present experimental method for the correction of X-ray intensities for TDS avoids complicated calculations and does not require knowledge of the elastic characteristics of the crystal. These characteristics are not known for most compounds, and particularly not at the temperature of the X-ray experiment. The problem is described by Stash & Zavodnik (1996) and Tsirelson & Ozerov (1996). The experimental approach to the TDS correction follows the methods of Jennings (1970) and Blessing (1987) and consists of the analysis of the profile of the diffraction peak near the peak–background boundaries and the modeling of the TDS contribution using analytical functions. The existing correction methods have a few drawbacks: (i) they have low statistical significance as they are applied to individual reflections; (ii) the physical components of the diffraction peak are described with low accuracy; (iii) the methods are usually not applicable to reflections with an unresolved $K\alpha_1$–$K\alpha_2$ doublet.

Stash & Zavodnik (1996) suggested an experimental approach which is free from the disadvantages mentioned above. The main feature of the method is that the standard peak profile, assumed for a small interval in diffraction angle, is the average of a number of peak profiles instead of the profile of an individual reflection; as a result, the statistical precision of the 'net' intensity determination increases greatly. Any prior knowledge about the shape of the diffraction peak or its components is not required; only the experimental information is used for this purpose. A short outline of the method is presented below.

The profiles of diffraction intensity peaks are treated with a special procedure (Streltsov & Zavodnik, 1989) which increases the statistical significance of the data. It

is applied when all the data are collected. At the outset, the whole 2θ range is divided into m intervals of width Δ_k ($\Delta_k = 5°$ for Mo $K\alpha$) and 'strong' reflections are chosen inside each interval. The criteria for inclusion of a reflection are based on the ratio of the scan speed of the reflection to that of the weakest observable reflection in the range and on the $I/\sigma(I)$ ratio. The peak boundaries are determined by the Lehmann & Larsen (1974) method for the selected reflections. The fact that the TDS peak is wider than the Bragg peak is reflected by a greater increase of the boundaries of the experimental peak profile with scattering angle than would follow from the 2θ spectral broadening. The background is subtracted and the profiles are normalized to unity and averaged within each interval. Simultaneously, the variances of the intensity at the points of these profiles are estimated. After this, the normalized peaks, $\hat{I}_k^{\mathrm{norm}}(2\theta)$, are used for the determination of the intensities and their variances of weak reflections in interval Δ_k. Stationary background measurements are not needed in this case and the correct estimation of 'net' intensity variances is achieved. As a result, the total set of TDS-uncorrected 'net' intensities and their variances is available.

The method is based on the following considerations. The profiles of the X-ray reflections are convolutions of many functions of different nature. The instrumental, spectral, crystal-shape and mosaicity functions *etc.* in a narrow section of reciprocal space remain the same, provided spectral broadening of the diffraction peaks is taken into account. Assuming the use of spherical crystals, the directional dependence of the reflections in reciprocal space can be ignored. Since the low-angle reflections are practically free from TDS, $\hat{I}_k^{\mathrm{norm}}(2\theta)$ of a low-order interval can be used as a 'reference' in the treatment of a high-angle reflection peak in order to describe its Bragg component. To do so, the profiles have to be expressed as function of equidistant points on the θ axis.

The 'net' profile of any reflection is a sum of $K\alpha_1$ and $K\alpha_2$ components, each containing a Bragg and a TDS contribution. The ratio of the intensity of the Bragg parts of the components is known (2.0 for Ag, Mo, and Cu radiation; *International Tables for Crystallography*, 1995, Vol. C). The assumption that the ratio of the $K\alpha_1$ to $K\alpha_2$ intensities for the TDS is the same as the ratio for the corresponding Bragg intensities allows the construction of a 'model peak', a description of the normalized and averaged experimental peak profile in each of the θ intervals. This contains only one adjustable parameter (the TDS contribution) according to

$$\hat{I}_k^{\mathrm{model}}(2\theta) = (1 - c_k)\hat{I}_k^{\mathrm{Bragg}}(2\theta) + c_k\hat{I}_k^{\mathrm{TDS}}(2\theta) \quad (1)$$

where k denotes the interval. The normalized Bragg and TDS profiles each consist of two contributions, one from the $K\alpha_1$ part of the incident beam and one from the $K\alpha_2$ part,

$$\hat{I}_k^{\mathrm{Bragg}}(2\theta) = I_{K\alpha_1}^{\mathrm{Bragg}}(2\theta) + I_{K\alpha_2}^{\mathrm{Bragg}}(2\theta)$$
$$\hat{I}_k^{\mathrm{TDS}}(2\theta) = I_{K\alpha_1}^{\mathrm{TDS}}(2\theta) + I_{K\alpha_2}^{\mathrm{TDS}}(2\theta). \quad (2)$$

It is assumed that the Bragg parts of the components have the same shape and width as the low-order reference reflection and that only the distance between the components along the θ scale differs. Stash & Zavodnik (1996) found that the profiles of the TDS parts $I_{K\alpha_i}^{\mathrm{TDS}}(2\theta)$ can be approximated in a simple and satisfactory way by the normalized parabolic functions

$$I_{K\alpha_i}^{\mathrm{TDS}}(2\theta) = b_0 - b_1(2\theta - 2\theta_i)^2 \text{ for } I_{K\alpha_i}^{\mathrm{TDS}}(2\theta) \geq 0$$
$$= 0 \text{ in all other cases} \quad (3)$$

in which b_0 and b_1 are constants and θ_i is the Bragg angle for the $K\alpha_i$ radiation. Again, only the distance between the components along the θ scale changes with θ. The boundaries l_1 and l_2 of the experimental peak are known from the profile analysis. The boundaries of the TDS peak profiles are symmetrical relative to the centers of the $K\alpha_1$ and $K\alpha_2$ peaks. The constant c_k, *i.e.* the TDS contribution in each interval, and the constants b_0 and b_1 are determined by the minimization of the functional

$$\Phi_\alpha = \sum_{i=I_1}^{I_2}[\hat{I}_k^{\mathrm{model}}(2\theta_i) - \hat{I}_k^{\mathrm{norm}}(2\theta_i)]^2. \quad (4)$$

The TDS coefficient α is determined as $\langle I^{\mathrm{meas}} \rangle = \langle I^{\mathrm{Bragg}} \rangle(1 + \alpha)$, where the terms in angled brackets refer to the integrated quantities. This leads to the relation

$$\alpha_k = c_k/(1 - c_k). \quad (5)$$

The set of $(m - 1)$ experimental α_k values gives the scattering-angle dependence of the full-range TDS correction. It is convenient then to fit these values to the function

$$a_2(\sin\theta_k/\lambda)^2 + a_3(\sin\theta_k/\lambda)^3 \quad (6)$$

with a_2 and a_3 as parameters. The measured intensities can now be corrected easily for TDS.

The method outlined was tested on a few crystals as described in detail by Stash & Zavodnik (1996) and the results were compared with the outcomes of theoretical calculations of TDS in the anisotropic two-phonon harmonic approximation, using elastic constants. From the good agreement between the results obtained by the two methods it was concluded that the experimental correction for TDS is correct.

References

Akselrud, L. G., Grin, Yu. M., Zavaly, P. Yu. & Pecharsky, V. K. (1990). The Second Conference on Accurate Structural Studies of Crystals, Riga, Abstract 158.

Bader, R. F. W. (1990). *Atoms in Molecules – A Quantum Theory.* Oxford University Press.

Becke, A. D. (1988). *Phys. Rev. A*, **38**, 3098–3103.

Becker, P. J. & Coppens, P. (1974). *Acta Cryst.* A**30**, 129–147.

Blessing, R. H. (1987). *Crystallogr. Rev.* **1**, 3–58.

Boek, E. S., Feil, D., Briels, W. J. & Bennema, P. (1991). *J. Cryst. Growth*, **114**, 389–410.

Bruning, H. & Feil, D. (1992). *Acta Cryst.* A**48**, 865–872.

Dirac, P. A. M. (1930). *Proc. Cambridge Philos. Soc.* **26**, 376.

Dixon, D. A. & Matzuzawa, N. (1994). *J. Phys. Chem.* **98**, 3967–3977.

Dovesi, R., Causa, M., Orlando, R., Roetti, C. & Saunders, V. R. (1990). *J. Chem. Phys.* **92**, 7402–7411.

Dovesi, R., Pisani, C., Roetti, C., Causa, M. & Saunders, V. R. (1989). *CRYSTAL*88. QCPE program 577, Bloomington, Indiana, USA.

Dovesi, R., Saunders, V. R., Roetti, C., Causa, M., Harrison, N. M., Orlando, R. & Aprà, R. (1996). *CRYSTAL*95 *User's Manual.* University of Torino, Torino, Italy.

Gatti, C., Saunders, V. R. & Roetti, C. (1994). *J. Chem. Phys.* **101**, 10686–10696.

Guth, H., Hegher, G., Klein, S., Treutmann, W. & Scheringer, C. (1980). *Z. Kristallogr.* **153**, 237.

Hansen, N. K. (1996). *SALLY.* Laboratoire de Cristallographie et Modélization des Matériaux Minéraux et Biologiques, Université Henri Poincaré, Nancy 1, France.

Hansen, N. K. & Coppens, P. (1978). *Acta Cryst.* A**34**, 909–921.

Hirshfeld, F. L. (1977). *Isr. J. Chem.* **16**, 226–229.

Howard, S. & Mallinson, P. (1993). *LSPROP*93. *Program for Topological Analysis of Charge Density.* Unpublished.

Jennings, L. D. (1970). *Acta Cryst.* A**26**, 613–622.

Lehmann, M. S. & Larsen, F. K. (1974). *Acta Cryst.* A**30**, 580–584.

Mullen, D. & Hellner, E. (1978). *Acta Cryst.* B**34**, 1624–1627.

Niu Jier (1994). PhD thesis, University of Siegen, Germany.

Perdew, J. P. & Wang, Y. (1986). *Phys. Rev. B*, **33**, 8800–8802.

Perdew, J. P. & Wang, Y. (1989). *Phys. Rev. B*, **40**, 3399.

Perdew, J. P. & Wang, Y. (1992). *Phys. Rev. B*, **45**, 13244–13249.

Protas, J. (1995). *MOLDOS*96/*MOLLY*. MS-DOS updated version (private communication).

Salahub, D. R., Proynov, E. I., Vela, A. & Ruiz, E. (1995). *New Methods in Quantum Theory*, NATO ASI Series, edited by C. A. Tsipis, V. S. Popov, D. R. Heishbach & J. S. Avery, pp. 359–398. Dordrecht: Kluwer Academic Publishers.

Scheringer, C., Mullen, D., Hellner, E., Hase, H. L., Schulte, K.-W. & Schweig, A. (1978). *Acta Cryst.* B**34**, 2241–2243.

Sheldrick, G. M. (1981). *SHELXTL User's Manual.* Nicolet XRD Corporation, Madison, Wisconsin, USA.

Spackman, M. A., Weber, H. P. & Craven, B. M. (1988). *J. Am. Chem. Soc.* **110**, 775–782.

Stash, A. I. & Zavodnik, V. E. (1996). *Crystallogr. Rep.* **41**, 404–412.

Stewart, R. F., Davidson, E. R. & Simpson, W. T. (1965). *J. Chem. Phys.* **42**, 3175–3187.

Streltsov, V. A. & Zavodnik, V. E. (1989). *Sov. Phys. Crystallogr.* **34**, 824–828.

Swaminathan, S., Craven, B. M. & McMullan, R. K. (1984). *Acta Cryst.* B**40**, 300–306.

Swaminathan, S., Craven, B. M., Spackman, M. A. & Stewart, R. F. (1984). *Acta Cryst.* B**40**, 398–404.

Tsarkov, A. A. & Tsirelson, V. G. (1991). *Phys. Status Solidi B*, **16**, 417–428.

Tsirelson, V. G. & Ozerov, R. P. (1996). *Electron Density and Bonding in Crystals.* Bristol, Philadelphia: IOP.

Velders, G. J. M. & Feil, D. (1993). *Theor. Chim. Acta*, **86**, 391–316.

Vosko, S. H., Wilk, L. & Nusair, M. (1980). *Can. J. Phys.* **58**, 1200.

Vries, R. Y. de (1996). PhD thesis, Twente University, Enschede, The Netherlands.

Worsham, J. E. Jr, Levy, H. A. & Peterson, S. W. (1957). *Acta Cryst.* **10**, 319–323.

Zachariasen, W. H. (1967). *Acta Cryst.* **23**, 558–564.